Original Paper

Audiology & Neurotology

Audiol Neurotol 2006;11:123–133
DOI: 10.1159/000090685

Published online: January 17, 2006

Magnetic Nanoparticles: Inner Ear Targeted Molecule Delivery and Middle Ear Implant

Richard D. Kopke[a, b, d] Ronald A. Wassel[a] Fadee Mondalek[c] Brian Grady[c]
Kejian Chen[a] Jianzhong Liu[a] Don Gibson[e] Kenneth J. Dormer[a, b]

[a]Hough Ear Institute, [b]Departments of Physiology and Otolaryngology, University of Oklahoma Health Sciences Center, Oklahoma City, Okla., [c]University of Oklahoma School of Chemical, Biological and Materials Engineering, Norman, Okla., [d]Oklahoma Medical Research Foundation, Oklahoma City, Okla., [e]NanoBioMagnetics Inc., Edmond, Okla., USA

Key Words
Magnetite · Superparamagnetic iron oxide nanoparticles · Therapeutic molecule delivery · Inner ear

Abstract
Superparamagnetic iron oxide nanoparticles (SNP) composed of magnetite (Fe_3O_4) were studied preliminarily as vehicles for therapeutic molecule delivery to the inner ear and as a middle ear implant capable of producing biomechanically relevant forces for auditory function. Magnetite SNP were synthesized, then encapsulated in either silica or poly (D,L,-Lactide-co-glycolide) or obtained commercially with coatings of oleic acid or dextran. Permanent magnetic fields generated forces sufficient to pull them across tissue in several round window membrane models (in vitro cell culture, in vivo rat and guinea pig, and human temporal bone) or to embed them in middle ear epithelia. Biocompatibility was investigated by light and electron microscopy, cell culture kinetics, and hair cell survival in organotypic cell culture and no measurable toxicity was found. A sinusoidal magnetic field applied to guinea pigs with SNP implanted in the middle ear resulted in displacements of the middle ear comparable to 90 dB SPL.

Introduction

Superparamagnetic iron oxide nanoparticles (SNP) have multiple applications in biomedicine [Pankhurst et al., 2003; Gupta and Gupta, 2005; Neuberger et al., 2005]. Molecular-sized SNP can locate in proximity to a biological target, be derivitized to promote biocompatibility or interaction with target cells, and are susceptible to an external magnetic field gradient (Coulomb's Law). Since the first magnetic polymeric particles of the 1970s, numerous nano- and microparticles have been developed to deliver therapeutic substances to target sites. Recently, we considered the ear as an organ where nanotechnology may be applied in targeted delivery and ossicular biomechanics [Dormer et al., 2005; Mamedova et al., 2005].

Synthetic, γ-Fe_2O_3 (maghemite) or Fe_3O_4 (magnetite) particles with a core less than 15 nm in diameter will exhibit superparamagnetism. Their crystalline structure approaches that of a single domain and atomic (magnetic) moment, hence, SNP have no residual magnetic interaction in the absence of a magnetic field (unlike larger ferromagnetic particles). However, if SNP are placed in a magnetic field of strength H, the numerous separate atomic moments in the material contribute to their 'super'paramagnetic response. The magnetic field, magnetic induction, $B = \mu_o (H + M)$, where μ_o is the perme-

KARGER

Fax +41 61 306 12 34
E-Mail karger@karger.ch
www.karger.com

Accessible online at:
www.karger.com/aud

Richard D. Kopke, MD
Hough Ear Institute, 3400 N.W. 56th St.
Oklahoma City, OK 73112 (USA)
Tel. +1 405 943 1716, ext. 602, Fax +1 405 947 6226
E-Mail rkopke@houghearinstitute.com

ability of the material and the magnetization $M = m/V$ is the magnetic moment (m) per volume of material. All materials are magnetic to some extent and are classified by their susceptibility (χ) to an external magnetic field, where $M = \chi H$. The uniform dispersal of SNP in aqueous solutions is dependent on the magnetic field, susceptibility to that field and also is related to the zeta potential of the particles. For in vivo applications, organic coatings surrounding SNP are used to insure dispersion and prevent aggregation of particles, which would impede transport across cell membranes.

Steric stabilization of SNP solutions can be achieved by polymeric encapsulation. Poly (D,L,-Lactide-co-glycolide, PLGA) is one such (biodegradable) polymer, which can also bind therapeutic moieties [Panyam et al., 2003; Aubert-Pouessel et al., 2004; Bala et al., 2004; Funhoff et al., 2004; Jeong et al., 2004; Jiang et al., 2004; Kumar et al., 2004a, b; Panyam et al., 2004; Prabha and Labhasetwar, 2004; Gupta and Gupta, 2005; Yamamoto et al., 2005]. One procedure used to encapsulate PLGA involves a double-emulsion technique, a water-in-oil emulsion being created, followed by this emulsion being dispersed in water [Gupta and Gupta, 2005]. Previous examples using this technique have been described; however, water-dispersible SNP were used that, in general, seem to have poor SNP dispersion in the polymer. Based on fundamental colloid chemistry principles, an oil-dispersible SNP should have much better dispersion.

Mechanical forces imposed on SNP by external magnetic fields have been used to manipulate tissues in which they reside or are attached [Puig-De-Morales et al., 2001]. Silica-encapsulated SNP chronically implanted into the middle ear epithelium of guinea pigs respond to a sinusoidal electromagnetic field and can oscillate the ossicular chain at displacements comparable to hearing levels [Dormer et al., 2005]. Implantable middle ear hearing devices in various stages of development directly drive the ossicular chain for hearing amplification using piezoelectric, motor or electromagnetic actuators [Dormer, 2003]. However, otologic biomechanical applications of SNP have not yet been made.

Nanotechnology also may prove useful in inner ear medicine with recent better understanding of the pathologies of noise- [Kopke et al., 2002], toxin- [Ravi et al., 1995; Song et al., 1997], inflammatory-, viral- and immune-mediated injury [Adams, 2002; Ryan et al., 2002] and cell death processes [Huang et al., 2000] leading to new treatment approaches [Kopke et al., 2002; Seidman and Van de Water, 2003]. Genetic and trophic factor manipulations have enhanced repair processes of inner ear neurosensory epithelium [Kopke et al., 2001b; Izumikawa et al., 2005]. Also, new methods have been tested for inner ear drug delivery including middle ear perfusion, use of catheters and wicks for round window membrane (RWM), cochlea, and vestibule [Kopke et al., 2001a; Jones et al., 2004; Izumikawa et al., 2005].

Safe, precise delivery of potentially therapeutic molecules remains a current challenge in otology/neurotology. We have been examining a new approach to inner ear drug delivery: SNP being pulled by magnetic forces, carrying a therapeutic payload into the inner ear in minutes. The RWM uniquely serves as portal of entry to cells of interest, i.e. sensory hair cells (HC), supporting cells, neurons, stria vascularis tissues. Small molecules, peptides, proteins, and viruses have been shown to pass through the RWM [Witte and Kasperbauer, 2000; Korver et al., 2002; Suzuki et al., 2003; Wang et al., 2003]. However, the passage of these molecules can be inefficient and highly variable [Juhn et al., 1988; Hoffer et al., 2001]. Additionally, most of these experiments involving passage of larger molecules through RWMs have been done in small animals, but humans have RWMs that are five to six times thicker than these animal models. Therefore, the larger molecules may not traverse the thick human RWM without the use of additional forces. The purposes of the preliminary studies reported here were to determine the feasibility of driving SNP and a payload across the RWM and the feasibility of driving the ossicular chain at a useful level with SNP embedded into the ossicular epithelium using externally applied magnetic forces. Our initial results with in vitro modeling, organotypic culture modeling, in vivo studies, and evaluation with fresh human temporal bones suggest the following: (1) SNP can be pulled through a tripartite in vitro membrane model, living guinea pig and rat RWM, and fresh cadaver RWM in less than 60 min by a magnetic force of ~0.3 tesla; (2) the magnetic gradient-forced transport supersedes diffusion or active forces of RWM transport; (3) SNP and PLGA particles appear biocompatible to inner ear tissues and to the RWM; (4) a payload has also been transported across the RWM in vivo, and (5) a sinusoidal magnetic field applied to implanted SNP resulted in ossicular displacements comparable to 90 dB SPL.

Materials and Methods

Synthesis of Nanoparticles

Our initial synthesis of magnetite (Fe_3O_4) utilized a procedure modified from Massart [Massart, 1981; Lian et al., 2004] in which the magnetite was prepared in an atmosphere saturated with nitro-

gen [Dormer et al., 2005]. Silica was tested as a biocompatible encapsulant for the magnetite and as a means to prospectively add both steric stabilization and a surface for derivatization of the particles.

For polymeric encapsulation of SNP into a larger composite nanoparticle, we hypothesized that oleic acid-coated magnetite nanoparticles (Liquid Research Ltd., Bangor, UK) and PLGA (Absorbable Polymers International, Pelham, Ala., USA) could be combined using previously published emulsification chemistry [Gupta and Gupta, 2005]. PLGA nanoparticles were formed using a double emulsion solvent evaporation technique [Prabha et al., 2002]. Following formulation of PLGA nanoparticles, dynamic light scattering (DLS) measurements determined hydrated particle size dispersion (HPP5001 High Performance Particle Analyzer, Malvern Instruments, Malvern, UK). Electron micrographs were taken also to determine particle size (H7600 Transmission Electron Microscope, Hitachi, Pleasanton, Calif., USA).

Electron Spin Resonance Spectroscopy

Aqueous 5,5-dimethyl-1-pyrroline- N-oxide (DMPO) was reacted with activated charcoal and then filtered. A baseline curve was made with DMPO. To determine if silica-coated SNP had reactive iron surfaces, a Fenton-type reaction was performed with 10 m*M* H_2O_2 added to a solution containing the DMPO spin trap and the SNP. Interaction of the SNP with the Fenton system was tested under three conditions: (1) the DMPO spin trap with 10 m*M* H_2O_2; (2) the addition of the SNP to the DMPO + H_2O_2 reaction system above, and (3) a positive control obtained by adding 60 μl of ferrous sulfate to the reaction seen in system 2 above. Spectra were obtained with the basic reaction system with the addition of 60, 180, and 300 μl SNP added to DMPO + H_2O_2, respectively (NanoBioMagnetics Inc., Edmond, Okla., USA).

Cell Growth Kinetics

A cell culture study of particle biocompatibility was performed. Madin-Darby canine kidney epithelial cells (MDCK) were seeded on the mucosal side of a porcine small intestine submucosa (SIS) membrane (Cook Biotech, West Lafayette, Ind., USA) at a seeding density of 4.8×10^5 cells/cm^2. Dextran-coated SNP (Nanomag-D NH2, Micromod, Germany) were added to the growth medium of the MDCK cells (1 mg/ml). Cells were counted at days 1, 2, 3, 5, 7, 9, 11, and 14 using a hemocytometer (Fisher Scientific, Pittsburgh, Pa., USA). On each of these days, cells were counted in 3 separate wells (n = 3).

Organotypic Culture Biocompatibility

Biocompatibility of SNP and PLGA nanoparticles containing SNP was tested using exposure to organotypic cell cultures of Corti's organ. Corti's organ was explanted from postnatal day 3 mouse pups and cultured for 24 h with standard Dulbecco's Modified Eagle's Medium (DMEM) at 37°C in 5% CO_2 similar to previously described methods [Nicotera et al., 2004]. Next the DMEM was replaced with fresh medium containing SNP (100 μg/ml) or PLGA particles with oleic acid-coated SNP embedded (1 mg/ml, 100 μg/ml, 1 μg/ml). That medium was replaced with fresh particle-free DMEM after 48 h. SNP cultures were maintained for 3–7 days (8 cultures for each time point). The PLGA cultures (4 samples at each of the three concentrations) were maintained in culture for an additional 3 days.

On the last day, the tissues were fixed in 4% paraformaldehyde and stained with tetramethylrhodamine B isothiocyanate (TRITC)- or fluoroscein isothiocyanate (FITC)-phalloidin to identify HC, cuticular plates, and stereocilia bundles under a light microscope as previously described [Kopke et al., 1997]. Specimens were mounted in mounting medium for fluorescence (VECTOR H-1000) and examined under a fluorescence microscope (Olympus BX51) with appropriate filter sets (excitation, 540 nm; emission, 573 nm) for TRITC and FITC (excitation, 495 nm; emission, 520 nm). Each explant of Corti's organ was examined in its full length. HC were identified by the bright FITC/TRITC phalloidin staining of the HC stereocilia bundles and cuticular plates, whereas missing HC were identified by the absence of cuticular plates and stereocilia bundles and the formation of supporting cell scars.

Magnetic Transport – in vitro RWM Model

Figure 1a illustrates our in vitro RWM model, a tripartite cell culture membrane constructed and cultured as previously described except that MDCK and fibroblasts were used instead of smooth muscle and urothelial cells [Zhang et al., 2000]. First, epithelial cells (MDCK) were cultured on one side of a small intestine submucosal membrane (Cook Biotech, West Lafayette, Ind., USA). Next, SWISS 3T3 fibroblasts were cultured on the contralateral side of the SIS membrane and allowed 2 days to penetrate the membrane. MDCK were then cultured on the free membrane surface and allowed 5 days to become confluent, as confirmed by measuring increased transmembrane electrical resistance (Epithelial Volt-Ohmmeter, WPI Inc., New Haven, Conn., USA) across the membrane until a peak in resistance was measured on day 4 before conducting the experiments.

Solutions of dextran-coated SNP clusters, 130 nm average diameter, or PLGA-embedded SNP, 160 nm diameter (1 mg/ml concentration) were placed on the upper surface of the RWM model. Individual NdFeB cylindrical magnets (Magstar Technologies) 6.35 × 6.35 mm were positioned so the centers of adjacent magnets were 2 cm apart. A plastic holder (12.8 × 8.6 × 3.1 cm) positioned the magnets directly under the culture wells of a 24-well plate. The magnetic field density measured at the surface of each of these magnets using a gauss meter (Model 5080, SYPRIS, Orlando, Fla., USA) averaged 0.41 tesla.

The SIS membranes with cultured cells were harvested at day 7 and fixed in 10% formalin, placed in 3% agar and stored in 10% formalin for subsequent histological sectioning at 4–5 μm. Sections were stained with Masson's trichrome (fig. 1b) and observed under light microscopy for signs of toxicity and positions of SNP en passage through the RWM. Transmission electron micrographs were taken on the fluid under the culture well inserts to verify magnetic gradient-forced transport of SNP across the RWM model.

Magnetic Transport – in vivo RWM Models

Adult Sprague-Dawley rats (n = 8) or albino guinea pigs (*Cavia porcellus*; n = 3) (Harlan, Indianapolis, Ind., USA) were anesthetized with a ketamine/xylazine ratio of 100/10 mg/kg for rats and 70/7 mg/kg for guinea pigs, i.m. The bulla was opened to expose the RWM. SNP, either dextran-coated 130-nm clusters of 20–30 nm (NanomagD, Micromod GmbH, Rostock, Germany) or silica-coated, 20–30 nm in diameter from our own synthesis, or PLGA-embedded SNP 160 nm in diameter (1 mg/ml) were placed in the RWM niche (1 μl for rats, 3 μl for guinea pigs). The RWM of the experimental ear was positioned horizontally facing upwards

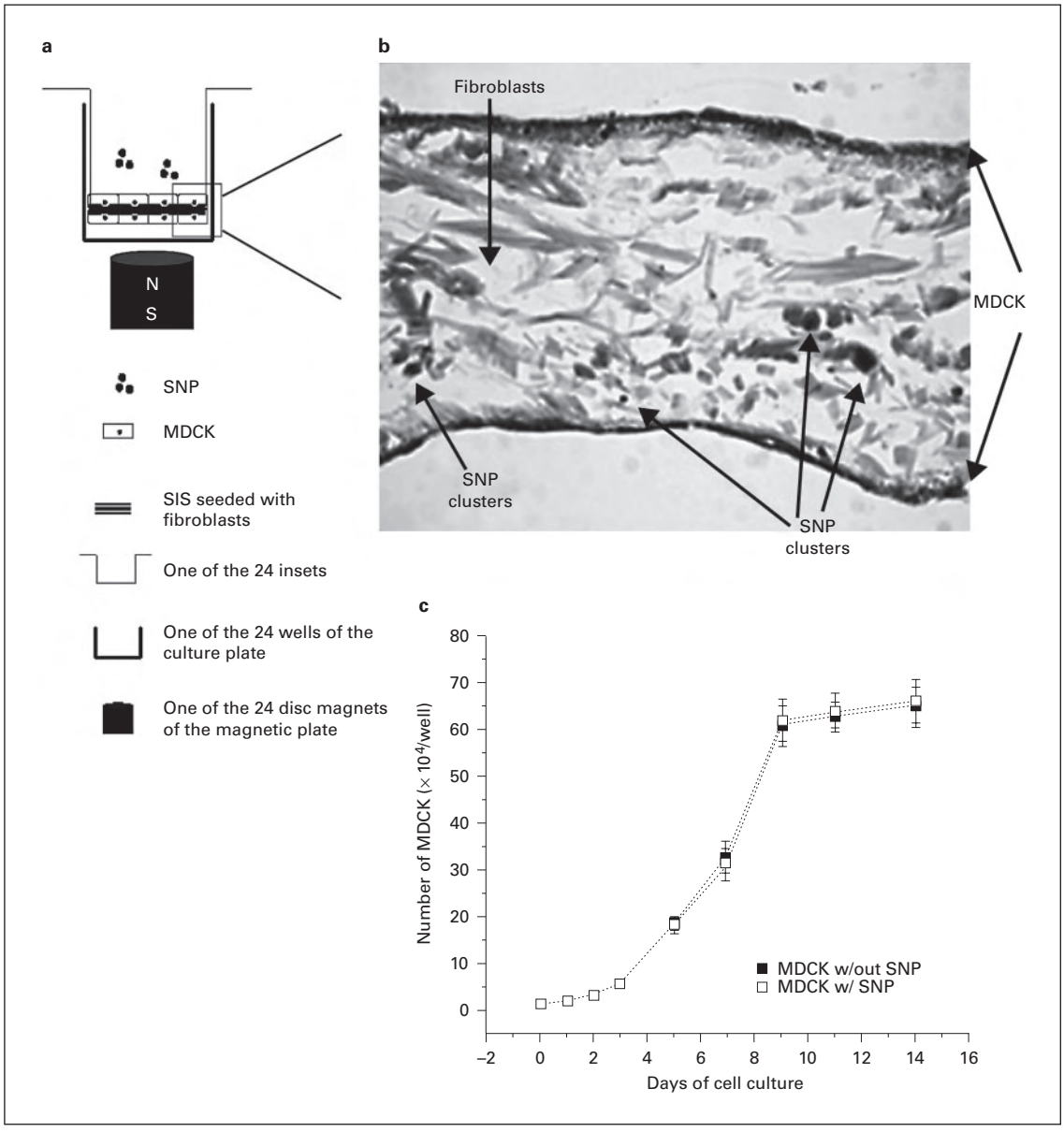

Fig. 1. a Schematic representation of 3 layers in the RWM model: a layer of fibroblasts sandwiched between 2 layers of MDCK cells. The diagram also shows the magnetic delivery system, a NdFeB magnet positioned under individual culture plate wells allowing for translational pulling of SNP across the membrane. **b** Photomicrograph of a cross-section of the RWM model showing stages of translational movement of the SNP. The cross-section shows MDCK cells on both sides of the SIS membrane and fibroblasts seeded within the SIS membrane. The SNP movement was captured on day 5 of cell culture. **c** Biocompatibility indicator growth plot showing that SNP (dextran-coated SNP, 1 mg/ml) have no effect on cell proliferation in MDCK cell culture. The cells were counted on days 1, 2, 3, 5, 7, 9, 11 and 14 of culture. Error bars represent standard deviation.

and the animal placed on the center surface of a 4-inch cube NdFeB48 magnet (Magnetic Sales, Culver City, Calif., USA). The distance from the RWM to the magnet pole face was 2.5 cm for rats and 3 cm for guinea pigs providing ~0.3 tesla for 20 min. The remaining SNP solution was then aspirated from the niche and replaced with a fresh solution (process was repeated two times for 60 min total exposure). Control animals went through the same protocol but without the magnetic field. The area of the basal turn and the apex, but not the RWM niche, was irrigated and aspirated dry. The bony wall on the basal turn of the cochlea was thinned

using an 18-gauge needle and a small hole made. A 30-gauge blunt-tip needle was inserted to the basal turn of the cochlea, and perilymph (10 μl for rats, 16 μl for guinea pigs) was withdrawn and saved for transmission electron microscopy (TEM). Fresh needles, syringes, and tubing were used for perilymph aspirations. The RWM was removed after fixation and also prepared for TEM.

The perilymph collected was washed twice with double-distilled water on a magnet to remove the salt content. The resulting 5-μl liquid was examined with TEM for nanoparticles. A small drop was put on glow-discharged formvar- and carbon-coated copper on nickel mesh grids. Samples were allowed to settle for 30 s, then wicked and rinsed 4 times with one drop of distilled/deionized water. RWM tissues were first rinsed in 0.1 *M* cacodylate buffer, then dehydrated through a series of acetones and finally rinsed in propylene oxide. After going through a series of propylene oxide/resin exchanges, samples were embedded in 8/2 resin. Transverse sections, 90 nm thick, were cut and put on 400 mesh copper grids that were glow discharged. Both perilymph and RWM samples were examined by TEM (H7600, Hitachi, Pleasanton, Calif., USA), and 2K × 2K digital images were taken (Megaplus ES 3.0, Advanced Microscopy Techniques, Danvers, Mass., USA). For each perilymph sample an average of 20 meshes from 2 grids were examined for nanoparticles. For RWM samples, 4 grids from each membrane sample were examined.

In order to quantify our observations for the guinea pig in vivo transport experiment, a 5-μl drop of control or magnet-exposed guinea pig perilymphatic fluid from a total of 2 animals was placed on the formvar grid. The particles evenly disperse and do not aggregate in fluid (data not shown). Fifteen randomly selected fields were observed and fifteen images were taken at 5000 × magnification, similar to figure 2g and i. The number of observed particles on each photograph was counted and compared between control and experimental samples. A two-tailed Student's t test was used to determine if the particle count means between the two samples were statistically different.

Magnetic Transport – Human Temporal Bone

SNP synthesized by NanoBioMagnetics Inc. were suspended in normal saline (0.2 mg/ml) and 5.5 μl was placed in the round window niche of human fresh frozen temporal bones (n = 2). Bones were placed approximately 1 inch from the pole face of a 4-inch cube NdFeB magnet external to the skull with the RWM parallel to the pole and exposed to approximately 0.3 tesla for 20 min. Next, the residual solution was removed from the niche and the procedure repeated twice for a total magnetic exposure of 60 min. After copious irrigation of the cochlear surface a cochleostomy was performed and 15 μl of perilymph aspirated using a 27-gauge needle and microsyringe for identification of SNP that were transported across the RWM. The same protocol was followed on a control temporal bone (no magnetic field). Both conventional TEM and electron energy loss spectroscopy (EELS) of particles prepared on formvar grids as previously described [Mamedova et al., 2005] were used to locate SNP in the sampled perilymphatic fluids. Conventional TEM techniques were used to locate approximately 10-nm electron dense spheres and confirm their elemental composition using the EELS feature searching at 708 eV for the iron L electron shell. The energy filtering option on the TEM microscope (CEM 902, Zeiss, Oberkochen, Germany) was used to photograph the iron-containing nanoparticles.

Ossicular Movements

SNP were silica coated and the silica surface was derivatized by the attachment of amino groups using 3-aminopropyltrimethoxysilane for conjugation with FITC [Dormer et al., 2005]. Intracellular location of fluorescent nanoparticles was subsequently done using scanning confocal microscopy. Guinea pigs were anesthetized and implanted with a sterile saline solution (50–75 μl) of SNP sonicated 3–4 min before placement either on the lateral wall of the surgically exposed incus (n = 9) or on the tympanic membrane (n = 2).

Each animal's head was laid on the pole face of a 4-inch cube NdFeB magnet (~0.30 tesla), the implanted ear facing up. Three aliquots of SNP were sequentially placed on the epithelium, then exposed to the magnet for 20 min. The animals recovered for 8–15 days and then were again anesthetized for laser Doppler single point interferometry measurements of velocity and conversion into displacements (Models OFV501 and 3000, Polytec PI, Tustin, Calif., USA) in response to an electromagnetic field. In a recumbent position, the incus was again exposed, and a 1 × 1-mm piece of reflective tape placed at the implant site. Interferometry measurements were made in response to a 6.5-mH coil activated at 500 or 1000 Hz, 5–8 V peak-to-peak (Model 80 Function Generator, Wavetek, San Diego, Calif., USA; Model 2706 Precision Amplifier, Bruel & Kjaer, Denmark).

Histological confirmation of the SNP implants was made by first decalcifying the incus, followed by transverse sectioning of the epithelium at 5 μm and observation using laser scanning confocal microscopy (Model TCS SP2, Leica, Mannheim, Germany).

Animal Care and Use

The experimental protocols were approved by the Institutional Animal Care and Use Committee, University of Oklahoma HSC. The study was performed in accordance with the Public Health Service Policy on Human Care and Use of Laboratory Animals, the National Institutes of Health Guide for the Care and Use of Laboratory Animals, the Animal Welfare Act and the principles of the Declaration of Helsinki.

Results

Synthesis of Nanoparticles

Figure 2a shows a TEM of PLGA particles. The PLGA particles had an average size of 99 ± 44 nm which was comparable with a size of 175 nm and a polydispersity index of 0.045 from DLS. Figure 2b shows a TEM of oleic acid-coated SNP incorporated into the PLGA microparticles. These particles had an average size of 85 ± 32 nm. The average size of the particles as measured via DLS was ~180 nm with a polydispersity index of ~0.1. The oleic acid-coated SNP appeared to range in size from 5 to 15 nm and incorporation of the SNP did not influence the size of the PLGA particles. As can be seen in figure 2c, the SNP have slightly aggregated together inside the polymer. This aggregation is most likely a result of the sonication process and not an artifact of evaporat-

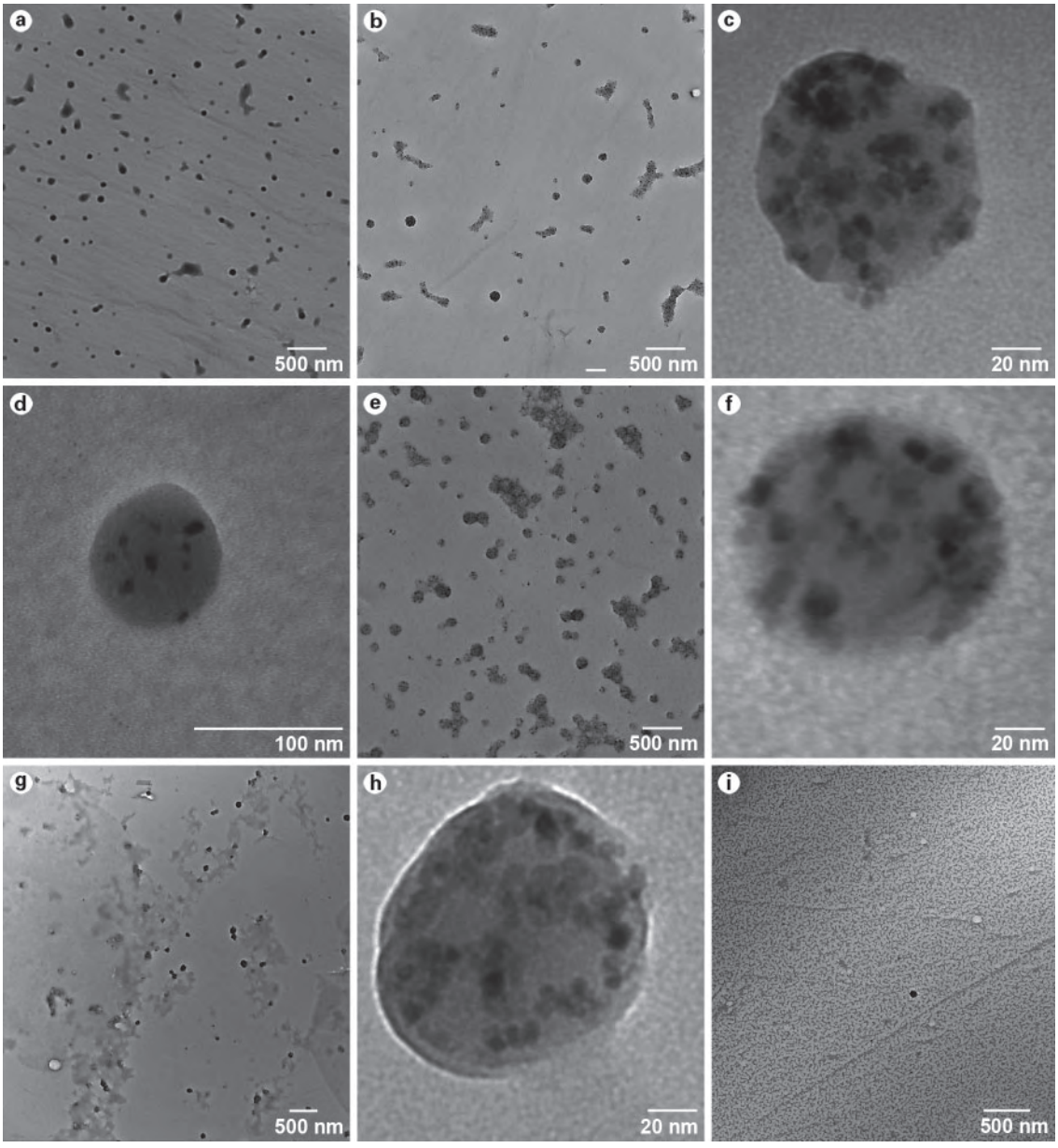

Fig. 2. TEM. **a** PLGA particles. Magnification 7000×. **b** PLGA particles with magnetite incorporated inside. Magnification 8000×. **c** PLGA particles with magnetite incorporated inside. Magnification 100000×. **d** PLGA particles made with a lower concentration of oleic acid-coated magnetite. Magnification 80000×. **e** PLGA particles with magnetite after passing through the RWM model. Magnification 7000×. **f** PLGA particles with magnetite after passing through the RWM model. Magnification 70000×. **g** PLGA particles with magnetite after passing through the RWM of a guinea pig. Magnification 5000×. **h** PLGA particles with magnetite incorporated inside from guinea pig perilymph. Magnification 100000×. **i** TEM of perilymphatic fluid from animal without magnet exposure demonstrating very few particles.

ing the particles on the TEM plate. The oleic acid-coated SNP embedded in the PLGA were not freely mobile. Thus aggregation of the magnetite is not expected when the particles are dried on the TEM grid. When a lower concentration of magnetite was used (1 vs. 5 mg/ml) in the formation of the PLGA microparticles, fewer magnetite particles were incorporated into the polymer and did not aggregate (fig. 2d).

Figure 2e, f shows TEM images of the magnetite-containing PLGA after having passed through the RWM model. TEM of a solution control experiment where no magnetic forces were employed demonstrated no particles in multiple TEM fields. In perilymphatic fluid samples from animals exposed to magnetic forces numerous particles were observed in multiple TEM fields as shown in figure 2g, h, whereas there were very few particles seen in fluid from animals not exposed to magnetic forces (fig. 2i). Quantitatively, the mean number of particles for the experimental (magnet exposed) sample was 51.2 ± 13.1 particles per photograph and the mean particle count for the control (no magnet exposure) samples was 1.8 ± 1.8 ($p < 0.001$).

Biocompatibility

ESR studies of silica-coated paramagnetic nanoparticles in a Fenton system revealed no evidence of free iron in the silica-encapsulated nanoparticles. There was no spectral evidence of free radical activity, supporting that the silica encapsulation of the nanoparticles prevented iron exposure and generation of free radicals.

As can be seen in figure 1c, the cell growth kinetics curve for MDCK cells grown in culture on SIS membranes was identical for cells cultured without particles or cells cultured with a concentration of 1 mg/ml of Nanomag-D NH_2 dextran particles.

Application of particles to organotypic cultures of mouse organ of Corti revealed little detectable HC loss or supporting cell scar formation with either the SNP (n = 8 at each time point) or the polymer-encapsulated oleic acid-coated paramagnetic nanoparticles (4 at each concentration). Very little or no HC loss was observed nor were replacement supporting cell scars detected (similar to control cultures not exposed to particles) at the light microscopic level in any of the cultures even at 1 mg/ml concentrations and at the longest time periods of culture. Representative photomicrographs of organotypic cultures are seen in figure 3.

TEM and light microscopy of explanted RWM (fig. 4a–c) and in vitro tripartite SIS membrane (fig. 1b), respectively, revealed no evidence of cell death, necrosis, inflammation or other obvious pathology on initial studies. Similar indicators of biocompatibility were noted for the particles incorporated in the middle ear mucosa of guinea pig ossicles [Dormer et al., 2005].

Magnetic Gradient Transport

A total of 9 SIS membrane inserts, 6 experimental and 3 controls, were utilized to assess magnetic gradient transport with and without magnetic forces. TEM observations detected a large number of SNP with a polymer payload in all 6 experimental inserts as seen in figure 2e, f. On the other hand, in the control membranes without magnetic forces no SNP were detected (data not shown). The concentration of SNP was 10^{12} particles/ml and 100 μl was applied to each insert.

TEM of fresh human cadaveric cochlear aspirate also readily demonstrated the particles of interest, whereas none were seen in the specimens not exposed to magnetic forces. These SNP were rapidly pulled through the human RWM in fresh frozen cadaveric human temporal bone and detected in the inner ear perilymphatic fluid. EELS confirmed that the particles contained iron. Perilymphatic fluid from temporal bones exposed to nanoparticles but no magnetic forces were devoid of these particles (fig. 5a, b).

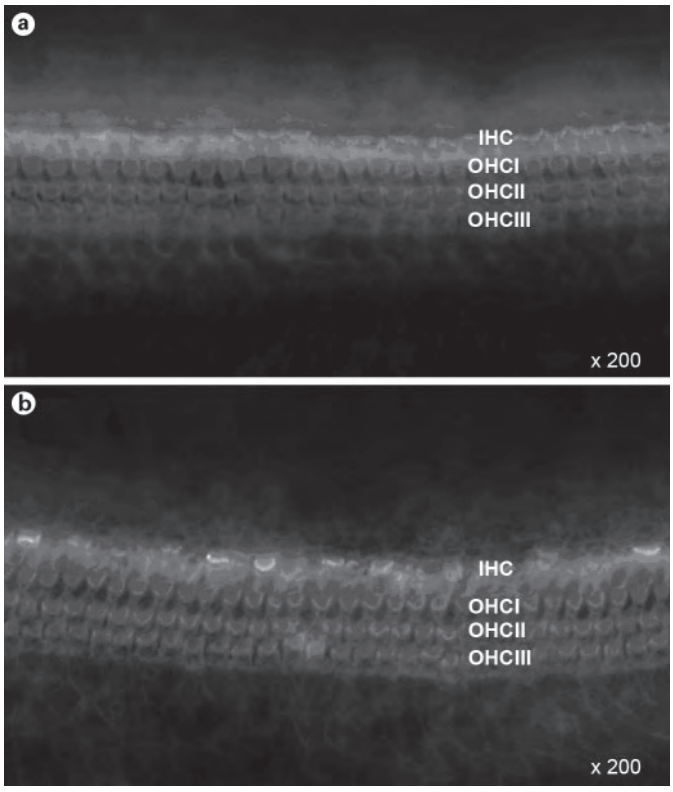

Fig. 3. Representative photomicrograph of cultured organ of Corti from postnatal day 3 mouse pups (5 days in vitro). Three rows of outer HC (OHC) and one row of inner HC (IHC) are shown. TRITC-phalloidin staining. **a** Control. **b** PLGA-SNP (1 mg/ml, 48 h) treated. At the light microscopic level, control and particle-exposed cultures all evidenced little, if any, HC loss. Magnification 200×.

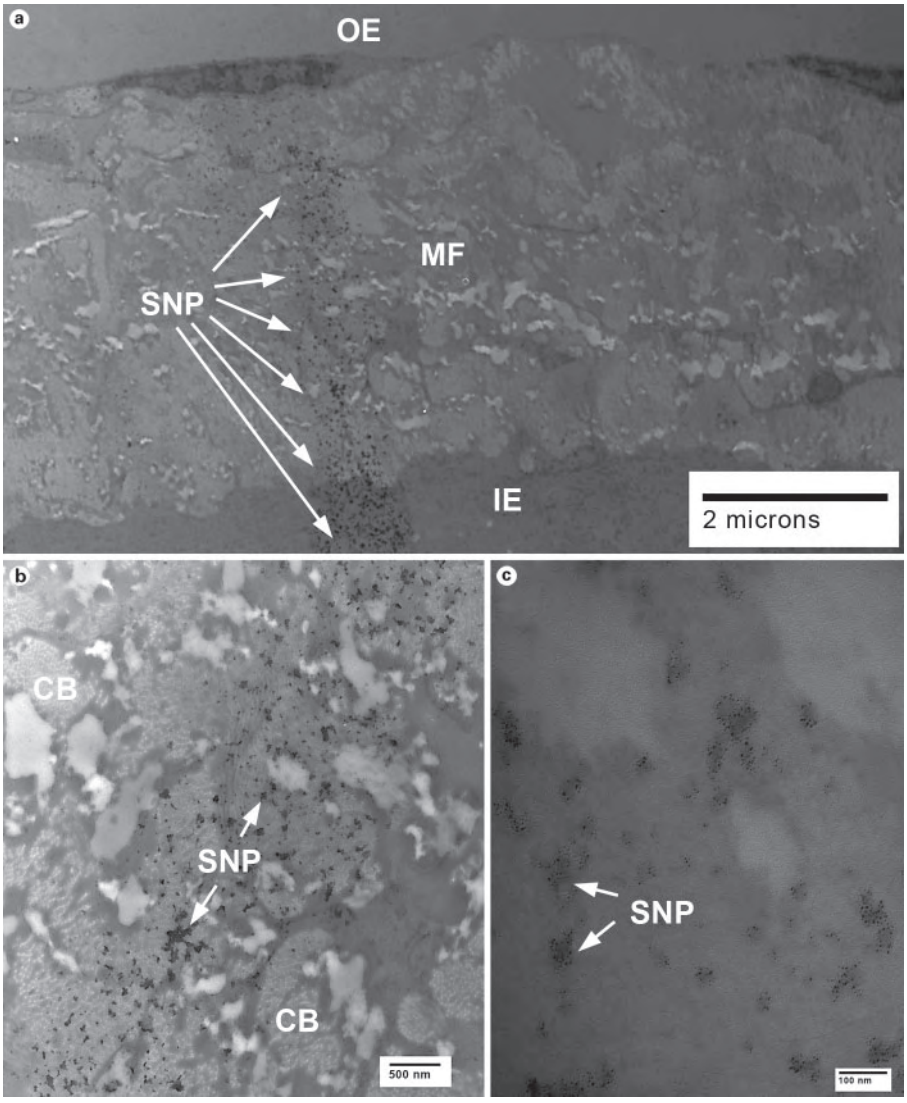

Fig. 4. SNP passing through RWM. TEM image of RWM from a rat exposed to magnet field for 60 min. Particles placed on the RWM in solution were drawn into and through the RWM with a magnetic gradient. Particles from samples from controls not exposed to magnetic forces were found only on the surface of the RWM (data not shown). **a** A low power magnification (1500×) view shows the RWM and SNP passing through three layers of the RWM (outer epithelium, middle fibrous layer, and into inner epithelium). **b** A high power view (6000×) shows the distribution of SNP within the RWM fibrous layer among collagen bundles. **c** A higher power view (40000×) shows the individual dextran-coated SNP clusters in the tissue. OE = Outer epithelium; MF = middle fibrous layer; IE = inner epithelium; CB = collagen bundle.

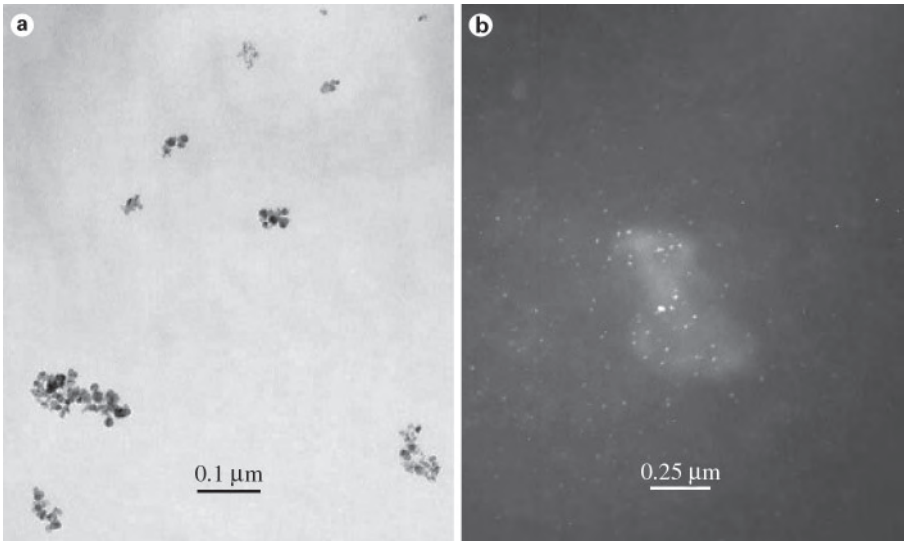

Fig. 5. These magnetic nanoparticles were rapidly pulled through the human RWM along a magnetic gradient in fresh cadaveric human temporal bone and detected in the inner ear perilymphatic fluid. **a** TEM of perilymphatic fluid aspirated from the cochlea of magnet-exposed temporal bone demonstrating particles. Original negative (85000×). **b** EELS confirms that the particles contain iron (bright dots). Perilymphatic fluid from temporal bone exposed to nanoparticles but no magnetic forces was devoid of these particles.

Ossicular Displacement

Silica-coated SNP, average diameter of 16 nm, with a zeta potential of –15 to –20 mV were internalized into epithelia of the tympanic membrane or that covering the incus. The density of SNP at the incus implant site was visible without magnification 8 days following implantation and the FITC-labeled SNP were visible under scanning confocal laser microscopy [fig. 6, 7 in Dormer et al., 2005]. Histopathology revealed no inflammatory response, no giant cells or evidence of apoptosis following 2–15 days of implantation. In this preliminary study, the displacements of the (intact) ossicular chain and tympanic membrane, as measured using single point interferometry, were comparable to 90 dB SPL displacements of the human middle ear [table 1, Dormer et al., 2005]. Frequency doubling occurred as the SNP responded to both polarities of the reversing electromagnetic field. This confirmed the superparamagnetic property of the magnetite SNP.

Discussion

The earliest use of external magnetic field to deliver clinical agents was in 1951, involving catheters for selective angiography. Magnetic microspheres were mostly studied until nanotechnology emerged in the late 1980s. Long-term deposition of iron in vivo is not a toxicity concern, as assessed epidemiologically in miners of hematite whose lung concentrations over lifetimes were 100–1000 times above those produced by drug targeting [Ranney, 1987]. Neither is adverse immunogenetic response a concern as iron is one of the most regulated cellular elements. Today, surface modifications can stabilize SNP in physiological solutions, protect against oxidation, provide functional groups for further derivitization and, in the case of polymeric encapsulation, carry and protect payloads en route to target tissues whereupon biodegradation will release payloads [Neuberger et al., 2005]. Future successes of SNP applications in nanomedicine, like other biomaterials, will be related to the extent of complete physicochemical characterizations (e.g. zeta potential) since surface chemistry dictates cell differentiation [Gupta and Gupta, 2005; Keselowsky and Garcia, 2005].

Middle Ear Biomechanics

For the first time it was shown that SNP, chronically implanted in a tissue, could be used to generate force, although performance data are lacking in this feasibility study [Dormer et al., 2005]. Current implantable middle ear hearing devices (IMEHD) under development or in clinical trials employ active electronic actuators consisting of motors, solenoid type drivers, piezoelectric crystals or magnets driven by an external magnetic field [Huttenbrink, 1999]. Reduced surgical and device risk, lower cost and direct drive benefit may be an advantage of tissue-indwelling, biocompatible SPN. Magnetite nanoparticles caused ossicular displacements in guinea pigs that were comparable to those in human temporal bones in response to a 90-dB SPL sound source. Nevertheless, the mass of the guinea pig ossicular chain is substantially less than in the human and was relatively easy to displace using an external magnetic field. Others have used magnetic particles to exert piconewton forces influencing (bone) cell differentiation [Cartmell et al., 2004]. RGD-coated microparticles bound to integrin receptors on primary human osteoblasts and an external magnetic field oscillated the cells in 2-D monolayer culture or 3-D constructs. Varying load-bearing matrices resulted.

Inner Ear Targeted Delivery

Of the prospective applications in nanomedicine, targeted delivery of therapeutics and enhanced MRI imaging, both utilizing nanoparticulate Fe_3O_4, may have the greatest clinical impact [Shinkai and Ito, 2004]. Delivering therapeutics only to target tissues may reduce both side effects and cost while improving treatment. Targeting of SNP by an external magnetic field had initially been explored for intravascular delivery. However, traversing the RWM provides a unique nanomedicine application where delivery particles will not be removed by reticuloendothelial organs. Like vascular targeting across the endothelium, inner ear delivery is independent of the membrane status and highly dependent on homogeneity of the magnetic field gradient in the target volume.

Substances with limited access to the inner ear may traverse (permeabilize) the RWM carrying a payload of drugs or genes to the inner ear. We have explored this targeted delivery for the first time utilizing SPN [Lee et al., 2004]. Our in vitro RWM model was used to initially identify candidate SNP for optimal targeted delivery to the inner ear (fig. 1a–c). In vivo testing in rat and guinea pig subsequently validated the RWM model, and we are currently refining the payload release from the biodegradable PLGA in perilymph. The model served to emulate the human RWM, penetrable to SNP, using external magnetic forces. Our results showed that cluster type aggregates (130 nm) containing 10 nm SPN were biocompatible and might be considered as carriers for therapeutic substances or as nonviral vectors for gene therapy. There

was no observable effect of the SPN on growth and proliferation of human epithelial cells in culture. The SPN crossed the tripartite RWM model much more rapidly than diffusion because of the forces from an external magnetic field. It is not surprising that a small number of particles were detected in perilymph of a guinea pig not exposed to magnetic forces since these particles are small enough to diffuse through the RWM or to be transported through active processes. However, the particles were much more evident after exposure to a magnetic gradient. Future studies are aimed at gathering additional quantitative information.

PLGA nanospheres have been used previously as nonviral vectors of DNA and other biologically active compounds. Labhasetwar and others tested biodegradable nanoparticles (~200 nm) consisting of PLGA and PVA [Panyam et al., 2002, 2004; Sahoo et al., 2004]. Particles have been loaded with wt-p53 plasmid DNA that transfected a breast cancer cell line [Prabha and Labhasetwar, 2004]. Sustained gene expression resulted from the slow intracellular release of the encapsulated DNA. Cellular uptake of PLGA particles 10–800 nm in diameter was confirmed by fluorescence of 6-coumarin and confocal microscopy [Qaddoumi et al., 2004]. Endocytosis appears to be involved in internalization and cationic surface treatment is facilitatory. PLGA nanoparticles (<200 nm) coated with a PVA-chitosan blend produce a cationic shell with the ability to electrostatically bind DNA to a nanosphere [Kumar et al., 2004a, b].

Therapeutic Perspectives

Inner ear medicine represents an expanding field that will benefit from improved targeted delivery strategies for a wide range of therapeutic small molecules, peptides, proteins, oligonucleotides and larger molecules containing genetic information. With the growing understanding of the molecular basis for traumatic, toxic, ischemic, inflammatory, infectious, and degenerative pathologies of the inner ear, specific efficient targeted delivery of mechanism-based therapeutics appears promising. In addition, plasmid gene delivery through an efficient, minimally invasive, safe method may increase the possibility of clinical auditory HC replacement with restoration of hearing. Here, in preliminary studies using materials comparable to those FDA approved and used clinically [Shinkai and Ito, 2004], we have demonstrated that readily achievable magnetic gradients can be created to enhance the delivery of paramagnetic nanoparticles with a biodegradable polymer payload into the mammalian inner ear.

Acknowledgements

Gratitude is expressed to Eric Howard, Associate Professor of Cell Biology, OUHSC, for his invaluable assistance in these ongoing studies.

This study was partially funded by The Shulsky Fund for Medicine and Research, New York City (via the Oklahoma City Community Foundation), the National Institute for Deafness and other Communicative Disorders (SBIR DC05528-01), the Office of Naval Research and INTEGRIS Baptist Medical Center, Oklahoma City.

K.J.D. and D.G. are stockholders in NanoBioMagnetics Inc.

References

Adams JC: Clinical implications of inflammatory cytokines in the cochlea: a technical note. Otol Neurotol 2002;23:316–322.

Aubert-Pouessel A, Venier-Julienne MC, Saulnier P, Sergent M, Benoit JP: Preparation of PLGA microparticles by an emulsion-extraction process using glycofurol as polymer solvent. Pharm Res 2004;21:2384–2391.

Bala I, Hariharan S, Kumar M: PLGA nanoparticles in drug delivery: the state of the art. Crit Rev Ther Drug Carrier Syst 2004;21:387–422.

Cartmell S, Magnay J, El Haj A, Dobson J: Use of magnetic particles to apply mechanical forces for bone tissue engineering purposes. Int Conf Fine Particle Magnetism, London 2004, pp 41–42.

Dormer KJ: Implantable electronic otologic devices for hearing restoration; in Finn WE, Lopresti PG (ed): Handbook of Neuroprosthetic Research Methods. Boca Raton, CRC Press, 2003, pp 237–261.

Dormer K, Seeney C, Lewelling K, Lian GD, Gibson D, Johnson M: Epithelial internalization of superparamagnetic nanoparticles and response to external magnetic field. Biomaterials 2005;26:2061–2072.

Funhoff AM, van Nostrum CF, Lok MC, Fretz MM, Crommelin DJA, Hennink WE: Poly(3-guanidinopropyl methacrylate): a novel cationic polymer for gene delivery. Bioconjug Chem 2004;15:1212–1220.

Gupta AK, Gupta M: Synthesis and surface engineering of iron oxide nanoparticles for biomedical applications. Biomaterials 2005;26:3995–4021.

Hoffer ME, Allen K, Kopke RD, Weisskopf P, Gottshall K, Wester D: Transtympanic versus sustained-release administration of gentamicin: kinetics, morphology, and function. Laryngoscope 2001;111:1343–1357.

Huang T, Cheng AG, Stupak H, Liu W, Kim A, Staecker H, Lefebvre PP, Malgrange B, Kopke R, Moonen G, Van de Water TR: Oxidative stress-induced apoptosis of cochlear sensory cells: otoprotective strategies. Int J Dev Neurosci 2000;18:259–270.

Huttenbrink KB: Current status and critical reflections on implantable hearing aids. Am J Otol 1999;20:409–415.

Izumikawa M, Minoda R, Kawamoto K, Abrashkin KA, Swiderski DL, Dolan DF, Brough DE, Raphael Y: Auditory hair cell replacement and hearing improvement by Atoh1 gene therapy in deaf mammals. Nat Med 2005, advanced online publication.

Jeong JR, Lee SJ, Kim JD, Shin SC: Magnetic properties of Fe_3O_4 nanoparticles encapsulated with poly(D,L-lactide-co-glycolide). IEEE T Magn 2004;40:3015–3017.

Jiang HL, Jin JF, Hu YQ, Zhu KJ: Improvement of protein loading and modulation of protein release from poly(lactide-co-glycolide) microspheres by complexation of proteins with polyanions. J Microencapsul 2004;21:615–624.

Jones GE, Jackson RL, Liu J, Costello M, Ge X, Coleman JKM, Boasen JF, Harper EA, Kuzdak NE, Kopke RD: Three methods of inner ear trophic factor delivery to recover vestibular function and morphology from gentamicin-induced vestibular toxicity in the guinea pig. Abstracts 27th Annu Midwinter Res Meet, Assoc Res Otolaryngol, Daytona Beach, 2004.

Juhn SK, Hamaguchi Y, Goycoolea M: Review of round window membrane permeability. Acta Otolaryngol Suppl 1988;457:43–48.

Keselowsky BG, Garcia AJ: Quantitative methods for analysis of integrin binding and focal adhesion formation on biomaterial surfaces. Biomaterials 2005;26:413–418.

Kopke RD, Coleman JK, Liu J, Campbell KC, Riffenburgh RH: Candidate's thesis: enhancing intrinsic cochlear stress defenses to reduce noise-induced hearing loss. Laryngoscope 2002;112:1515–1532.

Kopke RD, Hoffer ME, Wester D, O'Leary MJ, Jackson RL: Targeted topical steroid therapy in sudden sensorineural hearing loss. Otol Neurotol 2001a;22:475–479.

Kopke RD, Jackson RL, Li GM, Rasmussen MD, Hoffer ME, Frenz DA, Costello M, Schultheiss P, Van de Water TR: Growth factor treatment enhances vestibular hair cell renewal and results in improved vestibular function. Proc Natl Acad Sci USA 2001b;98:5886–5891.

Kopke RD, Liu W, Gabaizadeh R, Jacono A, Feghali J, Spray D, Garcia P, Steinman H, Malgrange B, Ruben RJ, Rybak L, Van de Water TR: Use of organotypic cultures of Corti's organ to study the protective effects of antioxidant molecules on cisplatin-induced damage of auditory hair cells. Am J Otol 1997;18:559–571.

Korver KD, Rybak LP, Whitworth C, Campbell KM: Round window application of D-methionine provides complete cisplatin otoprotection. Otolaryngol Head Neck Surg 2002;126:683–689.

Kumar M, Bakowsky U, Lehr CM: Preparation and characterization of cationic PLGA nanospheres as DNA carriers. Biomaterials 2004a;25:1771–1777.

Kumar M, Mohapatra SS, Kong X, Jena PK, Bakowsky U, Lehr CM: Cationic poly(lactide-co-glycolide) nanoparticles as efficient in vivo gene transfection agents. J Nanosci Nanotechnol 2004b;4:990–994.

Lee SJ, Jeong JR, Shin SC, Kim JC, Chang YH, Chang YM, Kim JD: Nanoparticles of magnetic ferric oxides encapsulated with poly(D,L lactide-co-glycolide) and their applications to magnetic resonance imaging contrast agent. JMMM 2004;272–76:2432–2433.

Lian G, Lewelling K, Johnson M, Gibson D, Dormer K, Seeney C: Fe_3O_4 magnetite nanoparticles coated by silica for biomedical applications. Microsc Microanal 2004;10(suppl 2):3.

Mamedova N, Kopke R, Liu J, Jackson R, Costello M, Gibson D, Dormer K: Feasibility of superparamagnetic nanoparticles for drug delivery to the inner ear. Abstracts 28th Annu Midwinter Res Meet – Assoc Res Otolaryngol, New Orleans 2005.

Massart R: Preparation of aqueous magnetic liquids in alkaline and acidic media. IEEE T Magn 1981;17:1247–1248.

Neuberger T, Schopf B, Hofmann H, Hofmann M, von Rechenberg B: Superparamagnetic nanoparticles for biomedical applications: possibilities and limitations of a new drug delivery system. JMMM 2005;1:483–496.

Nicotera TM, Ding D, McFadden SL, Salvemini D, Salvi R: Paraquat-induced hair cell damage and protection with the superoxide dismutase mimetic M40403. Audiol Neurootol 2004;9:353–362.

Pankhurst QA, Connolly J, Jones SK, Dobson J: Applications of magnetic nanopaticles in Biomedicine. J Phys D Appl Phys 2003;36:R161–R181.

Panyam J, Dali MA, Sahoo SK, Ma WX, Chakravarthi SS, Amidon GL, Levy RJ, Labhasetwar V: Polymer degradation and in vitro release of a model protein from poly(D,L-lactide-co-glycolide) nano- and microparticles. J Control Release 2003;92:173–187.

Panyam J, Williams D, Dash A, Leslie-Pelecky D, Labhasetwar V: Solid-state solubility influences encapsulation and release of hydrophobic drugs from PLGA/PLA nanoparticles. J Pharm Sci 2004;93:1804–1814.

Panyam J, Zhou WZ, Prabha S, Sahoo SK, Labhasetwar V: Rapid endo-lysosomal escape of poly(DL-lactide-co-glycolide) nanoparticles: implications for drug and gene delivery. FASEB J 2002;16:1217–1226.

Prabha S, Labhasetwar V: Nanoparticle-mediated wild-type p53 gene delivery results in sustained antiproliferative activity in breast cancer cells. Mol Pharm 2004;1:211–219.

Prabha S, Zhou WZ, Panyam J, Labhasetwar V: Size-dependency of nanoparticle-mediated gene transfection: studies with fractionated nanoparticles. Int J Pharm 2002;244:105–115.

Puig-De-Morales M, Grabulosa M, Alcaraz M, Mullol J, Maksym GN, Fredberg JJ, Navajas D: Measurement of cell microrheology by magnetic twisting cytometry with frequency domain demodulation. J Appl Physiol 2001;91:1152–1159.

Qaddoumi MG, Ueda H, Yang J, Davda J, Labhasetwar V, Lee VHL: The characteristics and mechanisms of uptake of PLGA nanoparticles in rabbit conjunctival epithelial cell layers. Pharm Res 2004;21:641–648.

Ranney DF: Magnetically controlled devices and biomodulation; in Tyle P (ed): Drug Delivery Devices. New York, NY, Marcel Dekker, 1988, pp 325–368.

Ravi R, Somani SM, Rybak LP: Mechanism of cisplatin ototoxicity – antioxidant system. Pharmacol Toxicol 1995;76:386–394.

Ryan AF, Harris JP, Keithley EM: Immune-mediated hearing loss: basic mechanisms and options for therapy. Acta Otolaryngol 2002;122:38–43.

Sahoo SK, Ma W, Labhasetwar V: Efficacy of transferrin-conjugated paclitaxel-loaded nanoparticles in a murine model of prostate cancer. Int J Cancer 2004;112:335–340.

Seidman M, Van de Water T: Pharmacologic manipulation of the labyrinth with novel and traditional agents delivered to the inner ear. Ear Nose Throat J 2003;82:276–280, 282–283, 287–288.

Shinkai M, Ito A: Functional magnetic particles for medical application. Adv Biochem Eng Biotechnol 2004;91:191–220.

Song BB, Anderson DJ, Schacht J: Protection from gentamicin ototoxicity by iron chelators in guinea pig in vivo. J Pharmacol Exp Ther 1997;282:369–377.

Suzuki M, Yamasoba T, Suzukawa K, Kaga K: Adenoviral vector gene delivery via the round window membrane in guinea pigs. Neuroreport 2003;14:1951–1955.

Wang J, Van de Water TR, Bonny C, de Ribaupierre F, Puel JL, Zine A: A peptide inhibitor of c-Jun N-terminal kinase protects against both aminoglycoside and acoustic trauma-induced auditory hair cell death and hearing loss. J Neurosci 2003;23:8596–8607.

Witte MC, Kasperbauer JL: Round window membrane permeability to transforming growth factor-alpha: an in vitro study. Otolaryngol Head Neck Surg 2000;123:91–96.

Yamamoto H, Kuno Y, Sugimoto S, Takeuchi H, Kawashima Y: Surface-modified PLGA nanosphere with chitosan improved pulmonary delivery of calcitonin by mucoadhesion and opening of the intercellular tight junctions. J Control Release 2005;102:373–381.

Zhang YY, Kropp BP, Moore P, Cowan R, Furness PD, Kolligian ME, Frey P, Cheng EY: Coculture of bladder urothelial and smooth muscle cells on small intestinal submucosa: potential applications for tissue engineering technology. J Urol 2000;164:928–934.